

Supplementary figures and tables for: A Bayesian source model for the 2004 great Sumatra-Andaman earthquake

Quentin Bletery,^{1,2} Anthony Sladen,¹ Junle Jiang^{3,4} and Mark Simons.³

¹Univ. Nice Sophia Antipolis, CNRS,
IRD, Observatoire de la Côte d’Azur,
Géoazur UMR 7329, 250 rue Albert
Einstein, Sophia Antipolis 06560 Valbonne,
France.

²Now at the Department of Geological
Sciences, University of Oregon, 1272
University of Oregon, Eugene, Oregon
97403, USA.

³Seismological Laboratory, Division of
Geological and Planetary Sciences,
California Institute of Technology,
Pasadena, California 91125, USA.

⁴Now at the Institute of Geophysics and
Planetary Physics, Scripps Institution of

References

- Banerjee, P., F. Pollitz, B. Nagarajan, and R. Bürgmann (2007), Coseismic slip distributions of the 26 December 2004 Sumatra-Andaman and 28 March 2005 Nias earthquakes from GPS static offsets, *Bulletin of the Seismological Society of America*, *97*(1A), S86–S102, doi:10.1785/0120050609.
- Bilham, R., R. Engdahl, N. Feldl, and S. P. Satyabala (2005), Partial and complete rupture of the Indo-Andaman plate boundary 1847-2004, *Seismological Research Letters*, *76*(3), 299–311, doi:10.1785/gssrl.76.3.299.
- Briggs, R. W., et al. (2006), Deformation and slip along the Sunda megathrust in the great 2005 Nias-Simeulue earthquake, *Science*, *311*(5769), 1897–1901.
- Gahalaut, V. K., B. Nagarajan, J. K. Catherine, and S. Kumar (2006), Constraints on 2004 Sumatra-Andaman earthquake rupture from GPS measurements in Andaman-Nicobar islands, *Earth and Planetary Science Letters*, *242*(34), 365–374, doi:10.1016/j.epsl.2005.11.051.
- Jade, S., M. B. Ananda, P. D. Kumar, and S. Banerjee (2005), Co-seismic and post-seismic displacements in Andaman and Nicobar Islands from GPS measurements, *Curr. Sci*, *88*(12), 1980–1984.
- Kreemer, C., G. Blewitt, W. C. Hammond, and H.-P. Plag (2006), Global deformation from the great 2004 Sumatra-Andaman earthquake observed by GPS: Implications for
-
- Oceanography, University of California San
 Diego, La Jolla, California 92093, USA.

- rupture process and global reference frame, *Earth, planets and space*, 58(2), 141–148.
- Meltzner, A. J., K. Sieh, M. Abrams, D. C. Agnew, K. W. Hudnut, J.-P. Avouac, and D. H. Natawidjaja (2006), Uplift and subsidence associated with the great Aceh-Andaman earthquake of 2004, *Journal of Geophysical Research: Solid Earth*, 111(B2), B02,407, doi:10.1029/2005JB003891.
- Smet, S., R. Michel, and L. Bollinger (2008), Uplift of the 2004 Sumatra-Andaman earthquake measured from differential hyperspectral imagery of coastal waters, *Journal of Geophysical Research: Solid Earth*, 113(B9), B09,403, doi:10.1029/2007JB005317.
- Subarya, C., M. Chlieh, L. Prawirodirdjo, J.-P. Avouac, Y. Bock, K. Sieh, A. J. Meltzner, D. H. Natawidjaja, and R. McCaffrey (2006), Plate-boundary deformation associated with the great Sumatra-Andaman earthquake, *Nature*, 440(7080), 46–51.
- Vigny, C., et al. (2005), Insight into the 2004 Sumatra-Andaman earthquake from GPS measurements in southeast Asia, *Nature*, 436(7048), 201–206, doi:10.1038/nature03937.

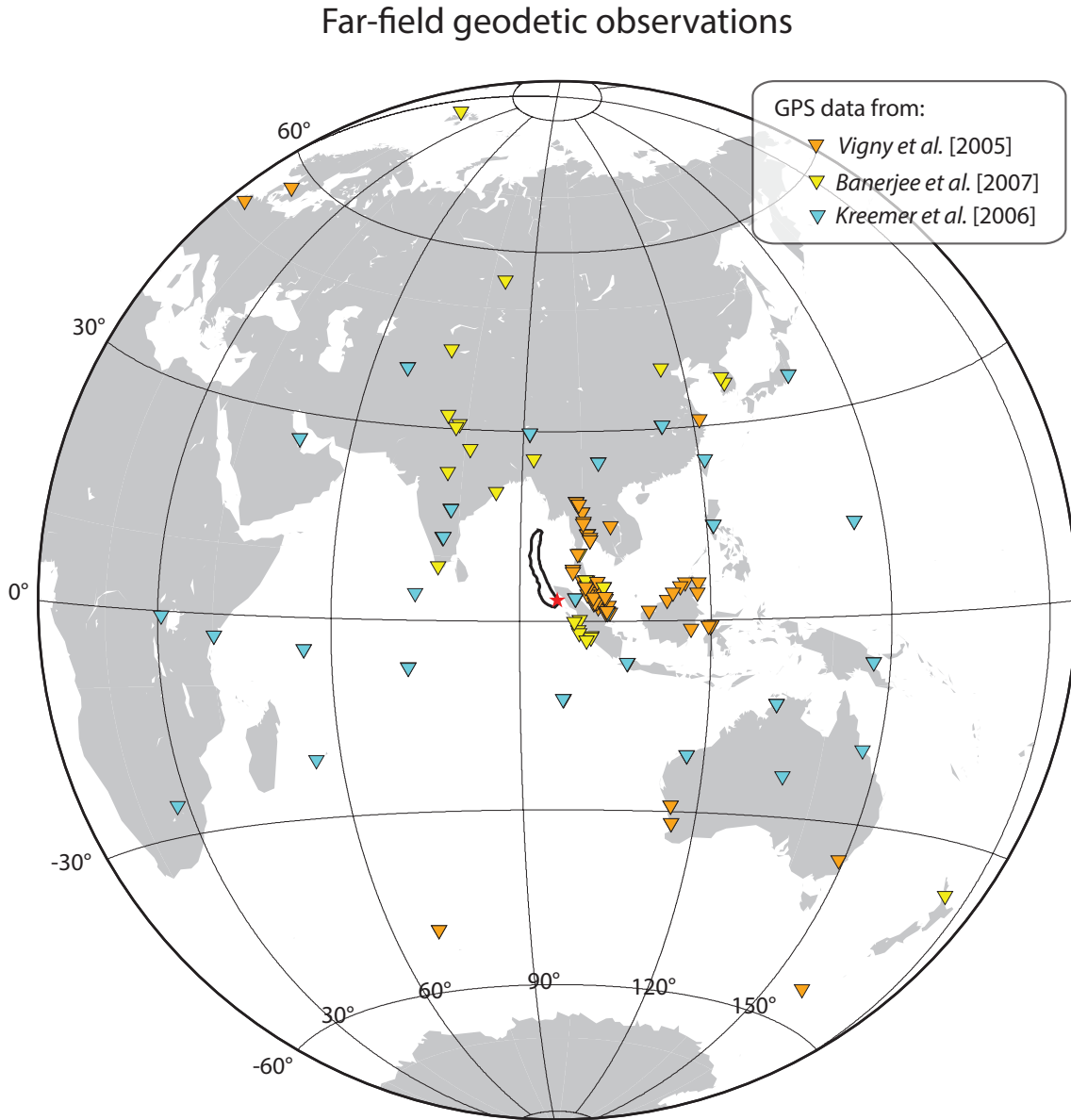


Figure S1. Far-field measurements of co-seismic offsets (horizontal only). Black contour is the suspected rupture area *Briggs et al.* [2006]. Red star is epicenter (USGS solution: earthquake.usgs.gov/earthquakes/eqinthenews/2004/us2004slav).

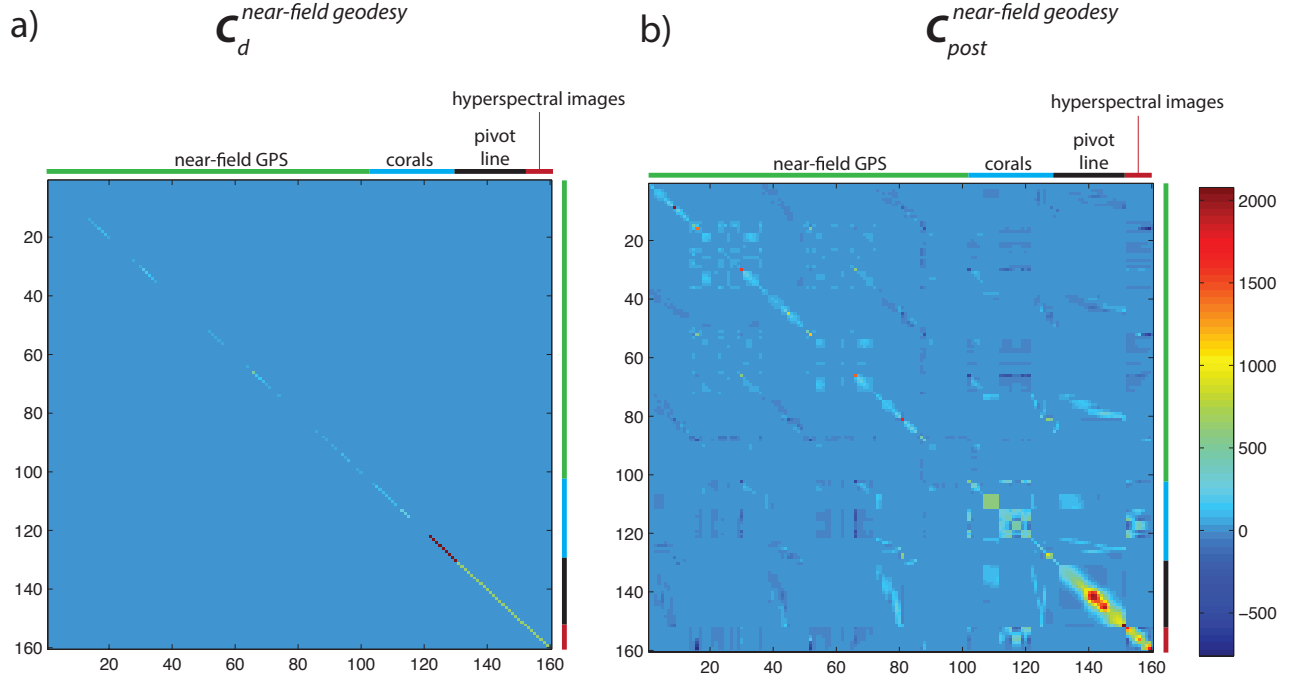


Figure S2. a) Covariance matrix \mathbf{C}_d^{geod} associated with error measurements on near-field geodetic data. b) Covariance matrix \mathbf{C}_{post}^{geod} associated with post-seismic contamination of the same near-field geodetic data. The color scale is saturated for both matrices at the maximum value of \mathbf{C}_{post}^{geod} .

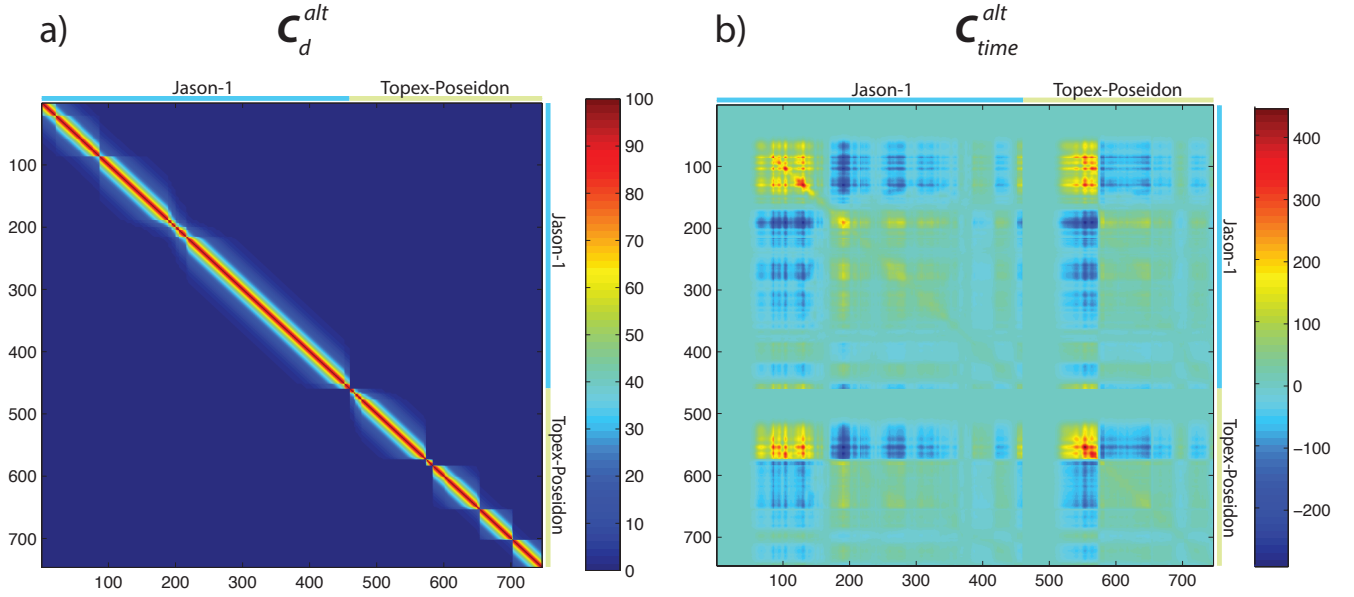


Figure S3. a) Covariance matrix C_d^{alt} associated with altimetry measurements. b) Covariance matrix C_{time}^{alt} associated with uncertainties on the kinematics of the rupture for the same altimetry data. We clearly see that the error on the altimetry estimates is dominated by the uncertainties on the rupture propagation (note the different color scale).

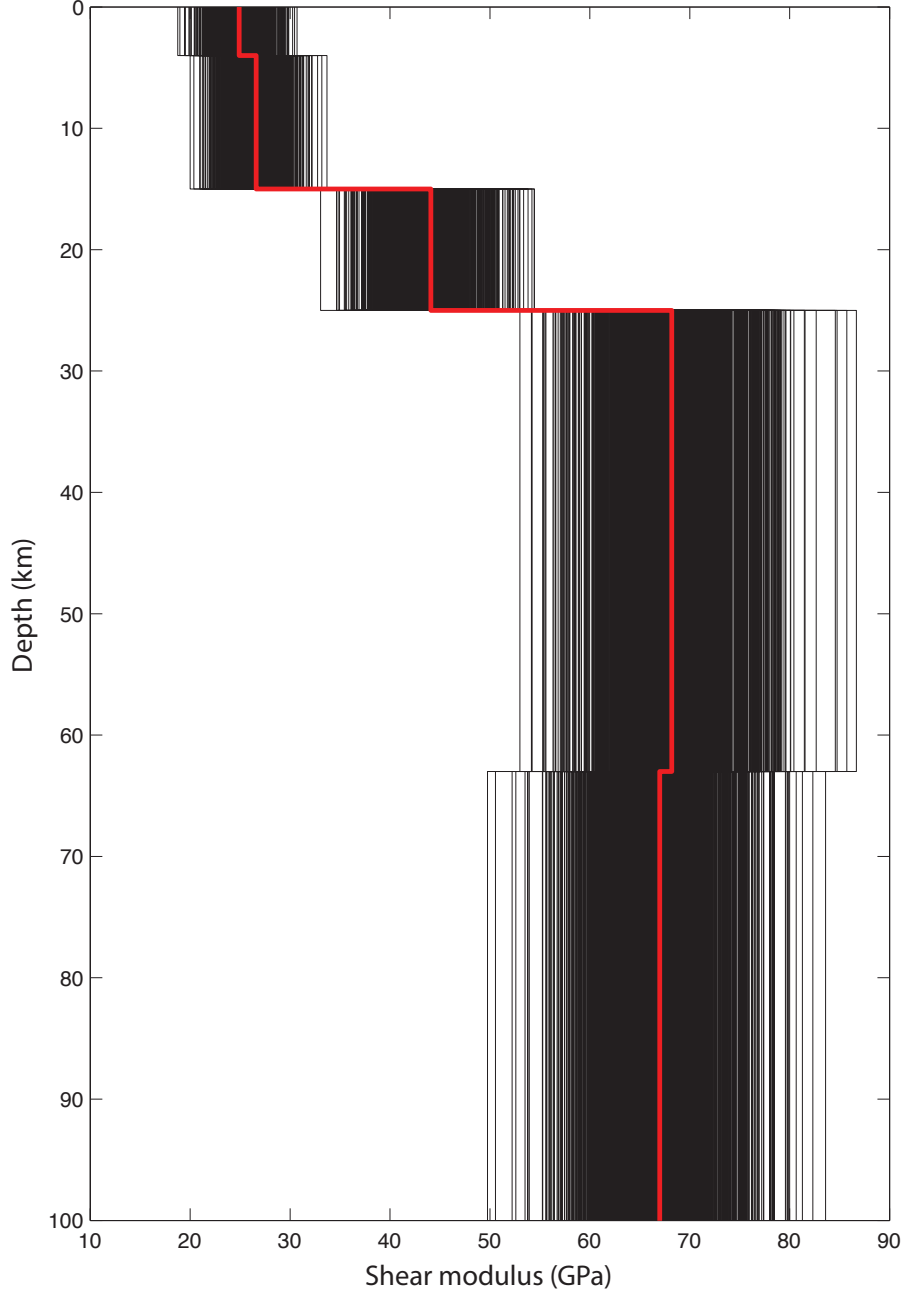


Figure S4. PREM (red) and Earth models space (grey) explored in the inversion process through the use of C_{earth} . The figure is obtained by drawing 1,000 stochastic models from the Gaussian distributions set in C_μ (with standard deviations equal to 8% of the μ values, see text).

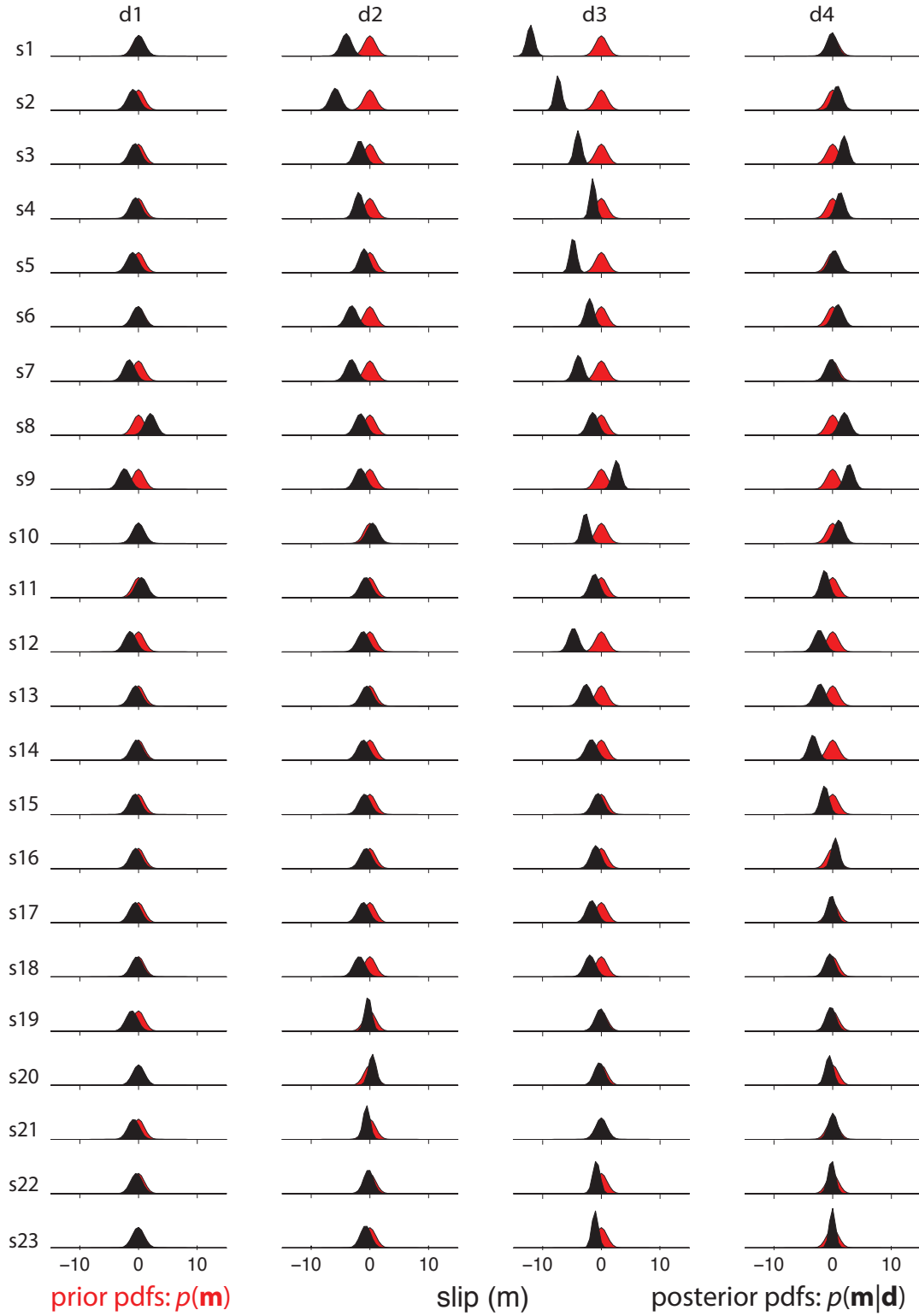


Figure S5. Prior (red) and posterior (black) probability density functions (PDFs) of the trench-parallel slip component. $s\#$ and $d\#$ labels indicate patch numbers along strike and dip directions, respectively. Consistently with labels in Figures 1 and 3, s1d1 corresponds

to the northern-most western-most patch, s23d4 to the southern-most eastern-most one.

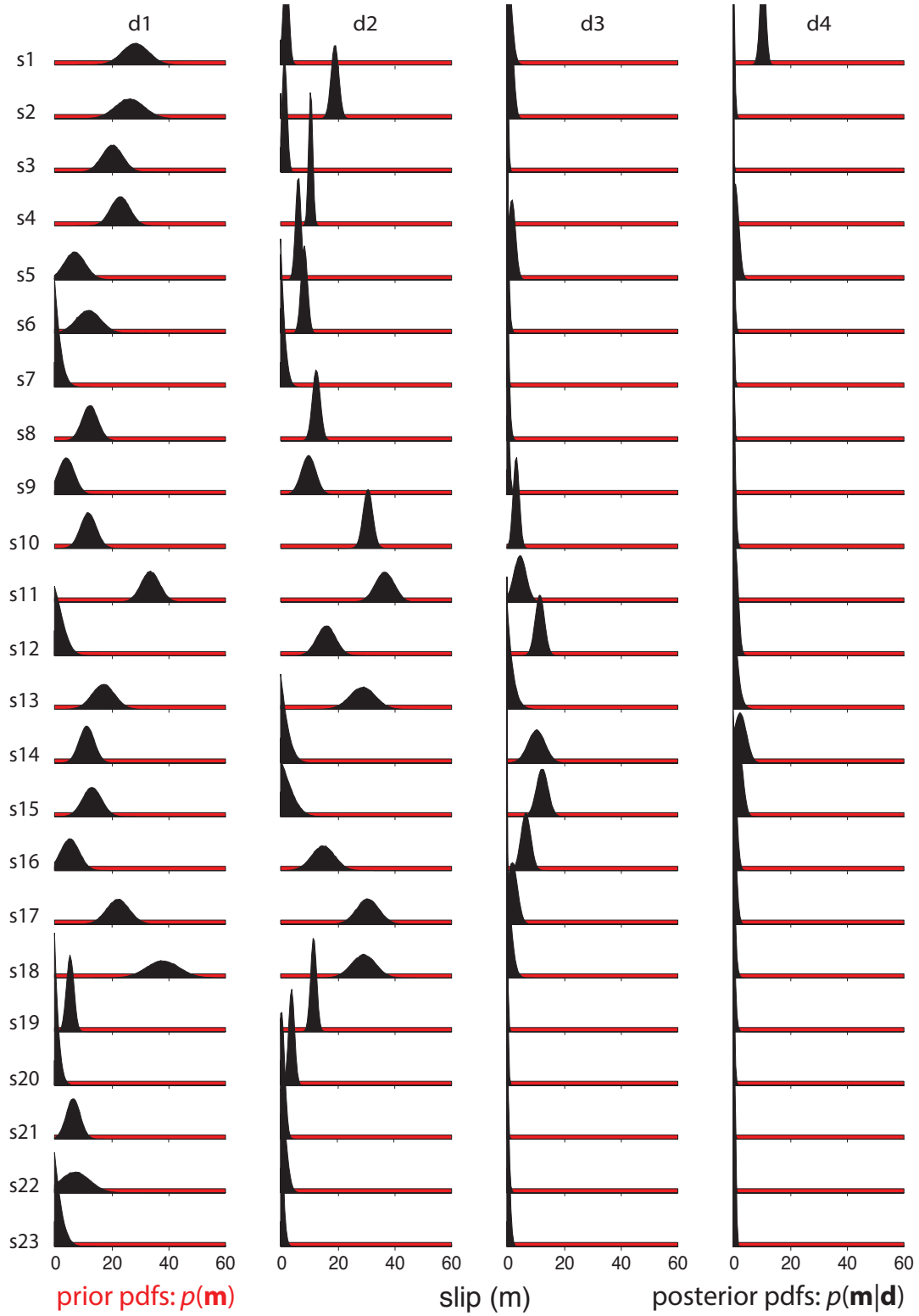


Figure S6. Prior (red) and posterior (black) PDFs of the trench-perpendicular slip component. PDFs disposition is the same as in Figure S5.

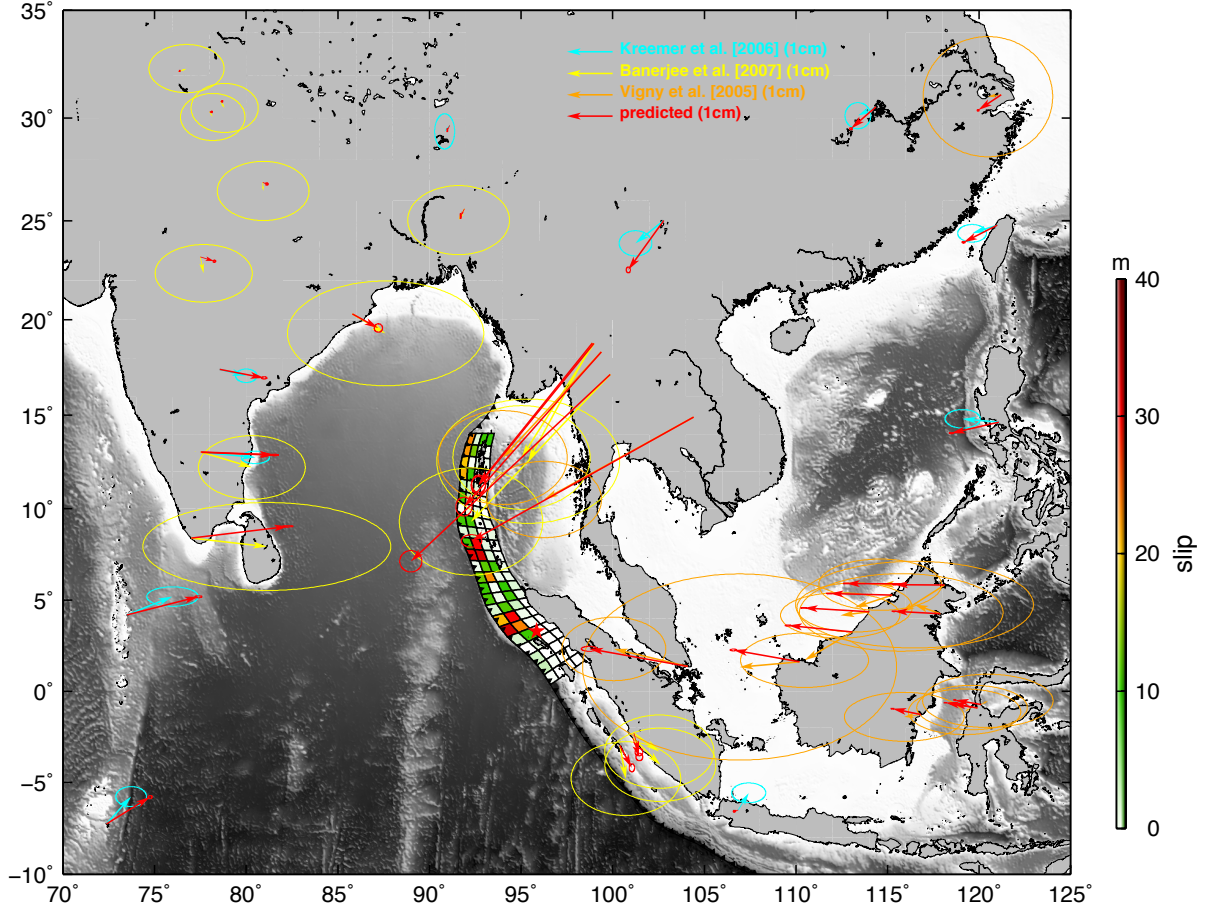


Figure S7. Fit of the far-field GPS data. Colors correspond to data source excepted for the red arrows which are the predictions for our average model. Red star is epicenter. Ellipses are $2\text{-}\sigma$ data and model uncertainties, expected for the red ones which are posterior variances as in Figure 4.

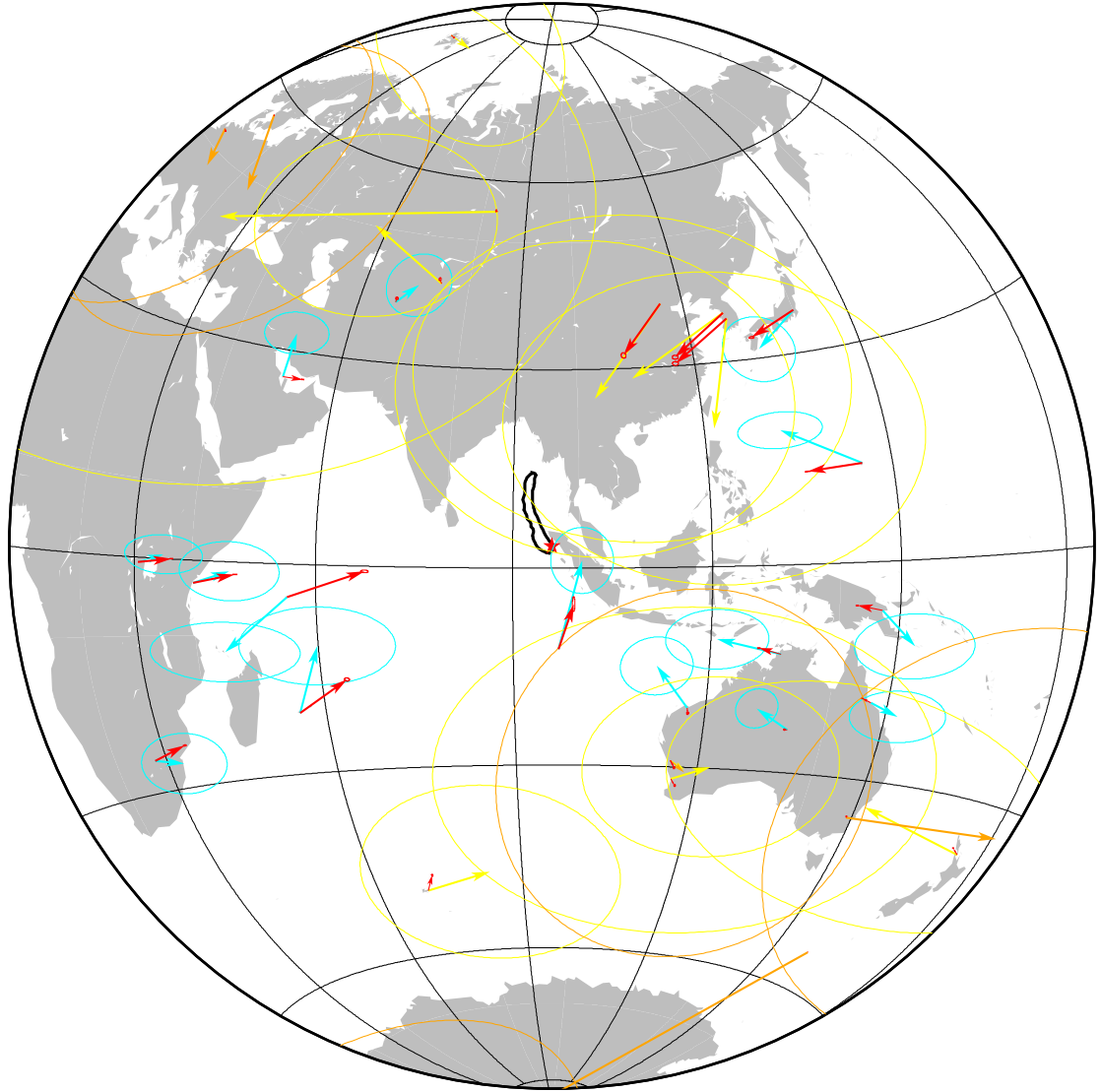


Figure S8. Fit of the very-far-field data. Red is predicted. Other colors correspond to data source as in Figure S1. Ellipses are $2\text{-}\sigma$ data and model uncertainties, expected for the red ones which are posterior variances as in Figure 4.

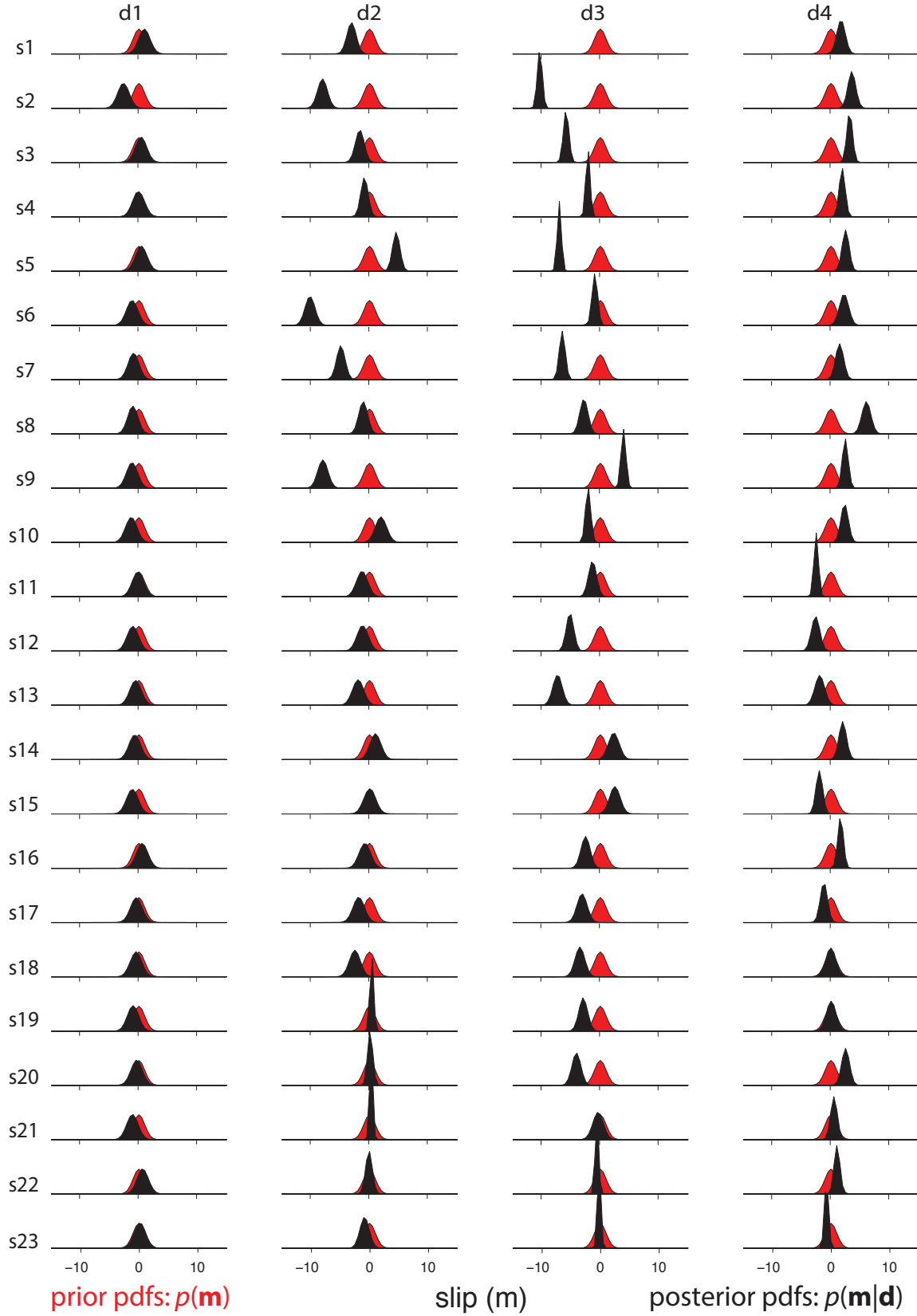


Figure S9. Same as S5 but only considering the diagonal terms of \mathbf{C}_d in the inversion.

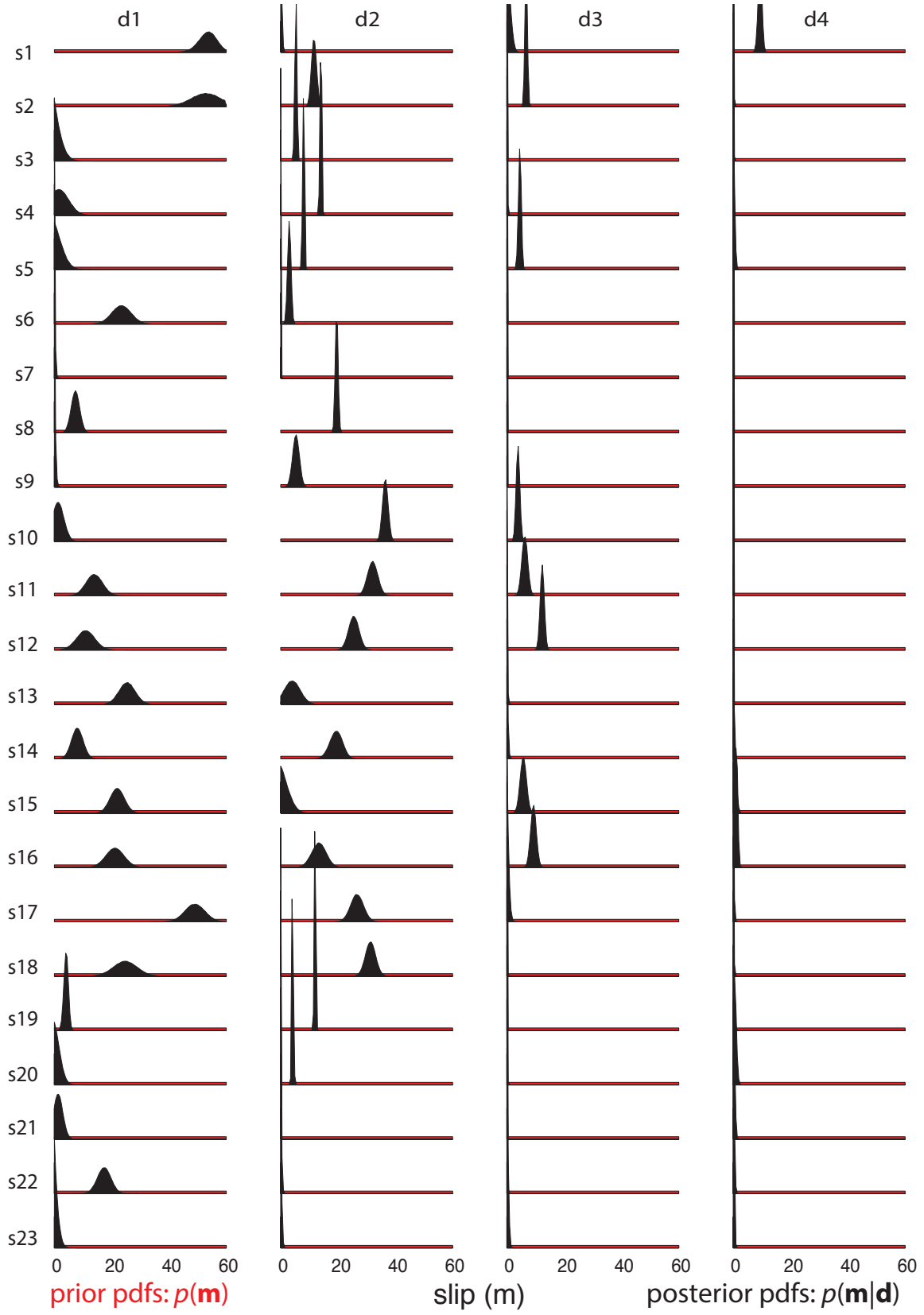


Figure S10. Same as S6 but only considering the diagonal terms of \mathbf{C}_d in the inversion.

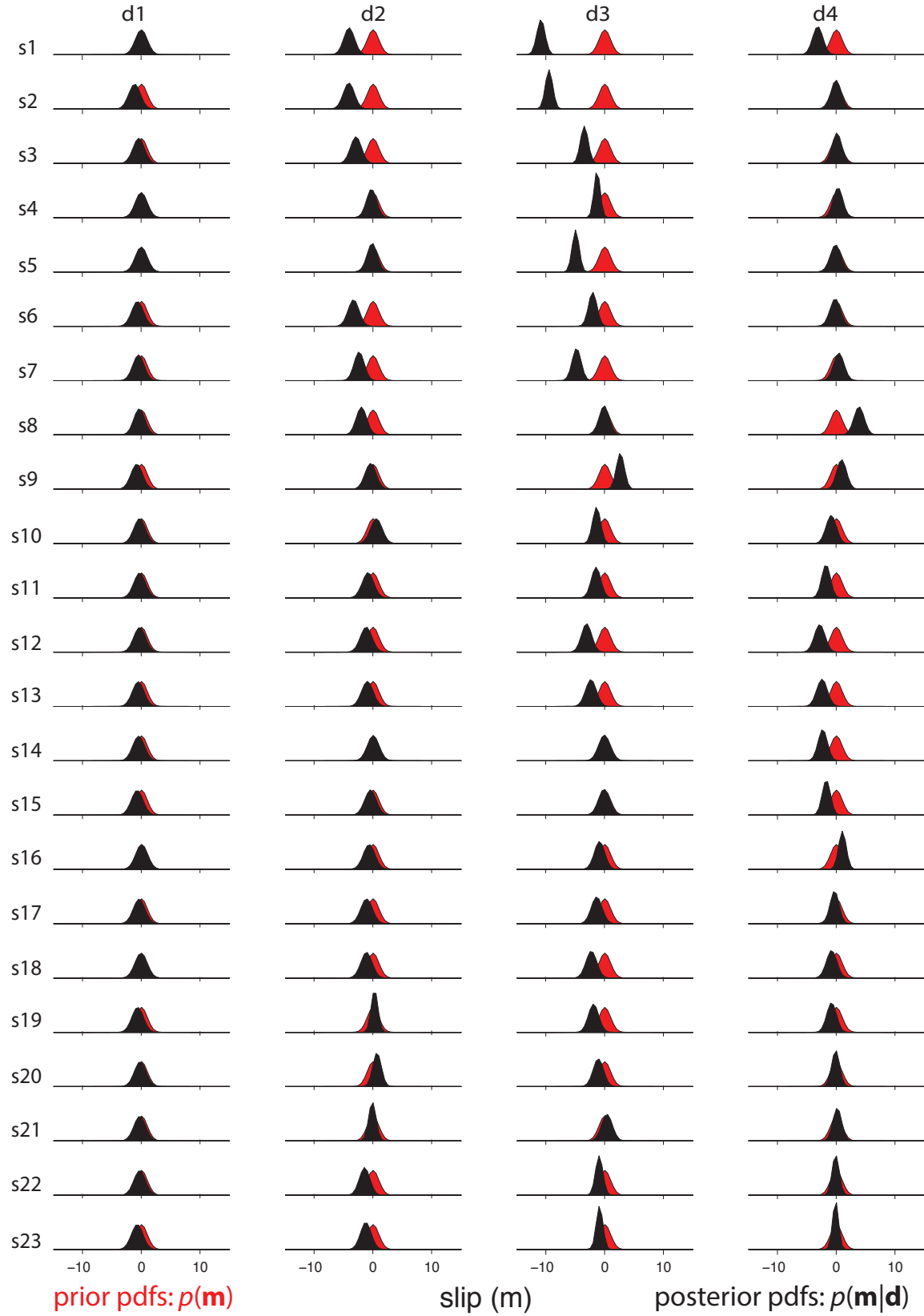


Figure S11. Same as S5 but only considering the diagonal terms of \mathbf{C}_χ in the inversion.

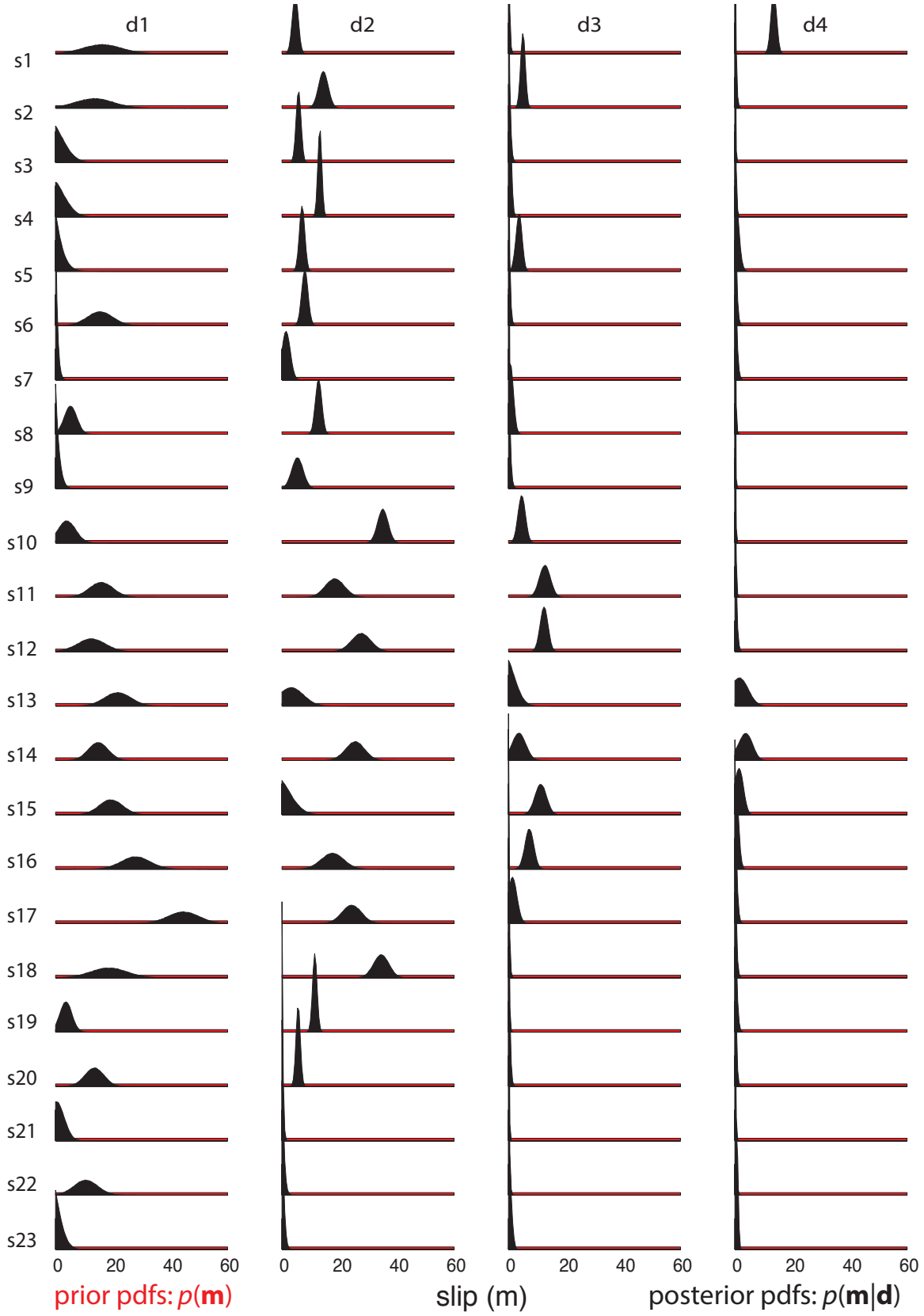


Figure S12. Same as S6 but only considering the diagonal terms of \mathbf{C}_χ in the inversion.

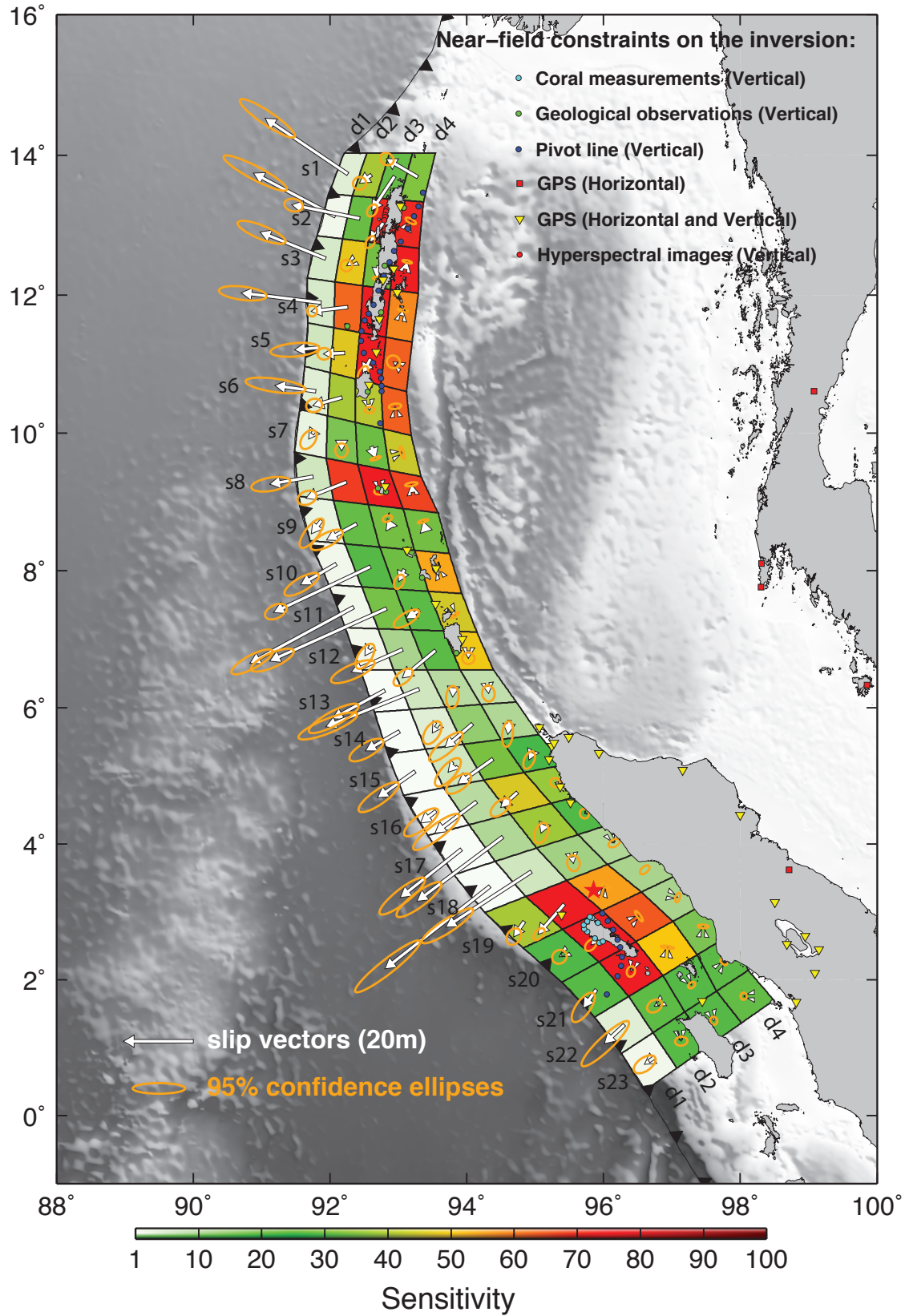


Figure S13. Sensitivity of the different dip-slip parameters to the geodetic dataset (L2 norm of the Green's functions columns normalized by the minimum sensitivity).

Table S1: Near-field GPS data included in the inversion. Tpost is the time of post-seismic displacements included in the observations. E, N, Z are offset measurements along east, north and the vertical component, respectively. eE, eN, eZ are the uncertainties associated with measurements on the different components.

Site	Lon	Lat	Tpost (days)	E (cm)	eE (cm)	N (cm)	eN (cm)	Z (cm)	eZ (cm)	Source
AB	93.027	13.278	20	-390	4	-271	1	49	5	<i>Gahalaut et al.</i> [2006]
EI	93.047	13.631	22	-362	4	-251	2	96	7	<i>Gahalaut et al.</i> [2006]
LI	92.932	12.376	20	-196	2	-110	1	-48	6	<i>Gahalaut et al.</i> [2006]
UG	92.773	12.216	20	-239	2	-166	1	-36	5	<i>Gahalaut et al.</i> [2006]
GG	92.983	12.036	21	-136	5	-95	2	-18	2	<i>Gahalaut et al.</i> [2006]
PB	92.721	11.649	16	-307	2	-103	1	-96	6	<i>Gahalaut et al.</i> [2006]
PI	92.676	11.178	27	-291	2	-119	1	-71	5	<i>Gahalaut et al.</i> [2006]
HB	92.569	10.696	23	-327	1	-265	1	-26	2	<i>Gahalaut et al.</i> [2006]
CN	92.804	9.225	58	-576	1	-295	1	-111	1	<i>Jade et al.</i> [2005]
TI	93.124	8.302	24	-586	2	-306	1	-285	4	<i>Gahalaut et al.</i> [2006]
KD	93.549	8.036	24	-397	2	-172	1	-135	4	<i>Gahalaut et al.</i> [2006]
MI	93.541	7.514	25	-491	2	-284	1	-216	5	<i>Gahalaut et al.</i> [2006]
CB	93.934	7.004	25	-410	2	-236	1	-160	3	<i>Gahalaut et al.</i> [2006]
BM12	98.945	2.6426	54	-8.9	6.66	-1.98	2.38	-8.05	7.33	<i>Subarya et al.</i> [2006]
D962	97.447	1.686	39	-3.32	6.49	-2.7	2.53	-5.35	5.58	<i>Subarya et al.</i> [2006]
D972	96.624	2.1744	43	1	6.69	-2.46	6.49	-57.14	6.69	<i>Subarya et al.</i> [2006]
JAHE	98.507	3.1452	53	-20.31	10.79	-2.18	8.82	0.53	8.99	<i>Subarya et al.</i> [2006]
K504	95.243	5.4338	40	-211.4	10.57	-176.34	8.82	-17.17	5.97	<i>Subarya et al.</i> [2006]
K505	95.272	5.48	39	-206.75	10.34	-174.55	8.73	-6.11	8.07	<i>Subarya et al.</i> [2006]
K515	95.487	5.5685	38	-165.99	8.3	-134.2	6.71	-4.62	6.37	<i>Subarya et al.</i> [2006]
LANG	98	4.4275	41	-36.81	4.11	-9.89	4.26	-1.19	6.08	<i>Subarya et al.</i> [2006]
LHOK	97.159	5.0866	36	-57.79	4.34	-21.9	4.78	7.65	10.54	<i>Subarya et al.</i> [2006]
MART	98.682	2.5242	55	-14.48	4.14	-1.27	2.4	-12.28	8.69	<i>Subarya et al.</i> [2006]
NIND	98.751	2.7295	56	-13.12	3.26	-0.65	2.3	-45.46	9.16	<i>Subarya et al.</i> [2006]
PAND	98.819	1.6759	33	-4.11	4.18	-3.55	3.97	-2.64	2.77	<i>Subarya et al.</i> [2006]
PIDI	95.933	5.3308	37	-139.93	4.05	-95.57	3.88	3.54	4.9	<i>Subarya et al.</i> [2006]
PISU	99.147	2.4476	55	-8.25	2.77	-1.43	3.11	-1.29	6.17	<i>Subarya et al.</i> [2006]
SIPA	99.089	2.1026	48	-10.27	6.62	-5.86	6.31	-11.44	6.99	<i>Subarya et al.</i> [2006]
TIGA	98.562	2.9186	55	-14.26	2.28	-0.41	2.36	4.52	3.05	<i>Subarya et al.</i> [2006]
R171	95.388	2.96	43	-382.09	8.59	-432.21	21.61	209.88	4.58	<i>Subarya et al.</i> [2006]
R173	95.518	4.607	39	-285.37	14.27	-237.63	11.88	-60.1	4.2	<i>Subarya et al.</i> [2006]

Table S1: Near-field GPS data included in the inversion. Tpost is the time of post-seismic displacements included in the observations. E, N, Z are offset measurements along east, north and the vertical component, respectively. eE, eN, eZ are the uncertainties associated with measurements on the different components.

R174	95.365	4.8419	40	-277.19	13.86	-241.43	12	-58.38	8.41	<i>Subarya et al.</i> [2006]
R175	95.203	5.2412	42	-243.49	12.17	-207.61	10.38	-22.66	12.11	<i>Subarya et al.</i> [2006]
R176	95.057	5.7129	45	-217.45	10.87	-171.09	8.55	-14.21	9.08	<i>Subarya et al.</i> [2006]
R178	95.333	5.8585	49	-158.85	7.94	-129.25	6.45	-	-	<i>Subarya et al.</i> [2006]
TELE	98.64	2.5349	55	-9.41	2.75	-0.26	2.29	-	-	<i>Subarya et al.</i> [2006]

Table S2: Near-field vertical offsets included in the inversion. Tpost, Z and eZ are defined in table S1.

Site	Lon.	Lat.	Tpost(days)	Z(cm)	eZ(cm)	Source
Smet1	92.826	13.23	47	112	10	<i>Smet et al.</i> [2008]
Smet2	92.818	13.20	47	89	10	<i>Smet et al.</i> [2008]
Smet3	92.808	13.15	47	80	10	<i>Smet et al.</i> [2008]
Smet4	92.808	13.12	47	77	10	<i>Smet et al.</i> [2008]
Smet5	92.795	13.07	47	56	10	<i>Smet et al.</i> [2008]
Cor1	95.763	2.709	41	131	5	<i>Subarya et al.</i> [2006]
Cor2	95.716	2.749	41	147	16	<i>Subarya et al.</i> [2006]
Cor3	95.714	2.807	41	148	16	<i>Subarya et al.</i> [2006]
Cor4	95.836	2.914	41	34	16	<i>Subarya et al.</i> [2006]
Cor5	95.872	2.613	41	101	5	<i>Subarya et al.</i> [2006]
Cor6	95.937	2.548	41	46	5	<i>Subarya et al.</i> [2006]
Cor7	95.992	2.569	41	48	5	<i>Subarya et al.</i> [2006]
Cor8	95.763	2.861	41	132	5	<i>Subarya et al.</i> [2006]
Cor9	95.918	2.844	41	22	5	<i>Subarya et al.</i> [2006]
Cor10	95.804	2.924	41	46	5	<i>Subarya et al.</i> [2006]
Bil1	93.08	13.25	20	70	100	<i>Bilham et al.</i> [2005]
Bil2	92.8	12.42	20	150	100	<i>Bilham et al.</i> [2005]
Bil3	92.25	11.55	20	150	100	<i>Bilham et al.</i> [2005]
Bil4	92.55	10.6	20	100	100	<i>Bilham et al.</i> [2005]
Bil5	92.75	11.75	20	-150	100	<i>Bilham et al.</i> [2005]
Bil6	92.7	9.2	20	100	100	<i>Bilham et al.</i> [2005]
Bil7	92.82	9.15	20	-100	100	<i>Bilham et al.</i> [2005]
Bil8	93.85	6.8	20	-150	100	<i>Bilham et al.</i> [2005]
Bil9	93.35	7.9	20	-200	100	R. Bilhams website
SatIm1	93.3610	13.4699	90	0	25	<i>Meltzner et al.</i> [2006]
SatIm2	93.2963	13.2714	90	0	25	<i>Meltzner et al.</i> [2006]
SatIm3	93.2304	13.1281	90	0	25	<i>Meltzner et al.</i> [2006]
SatIm4	93.1386	12.9497	90	0	25	<i>Meltzner et al.</i> [2006]
SatIm5	93.0316	12.7662	90	0	25	<i>Meltzner et al.</i> [2006]

Table S2: Near-field vertical offsets included in the inversion. Tpost, Z and eZ are defined in table S1.

SatIm6	92.9398	12.6337	90	0	25	<i>Meltzner et al.</i> [2006]
SatIm7	92.8685	12.4706	90	0	25	<i>Meltzner et al.</i> [2006]
SatIm8	92.7869	12.2718	90	0	25	<i>Meltzner et al.</i> [2006]
SatIm9	92.7105	12.0628	90	0	25	<i>Meltzner et al.</i> [2006]
SatIm10	92.6340	11.8589	90	0	25	<i>Meltzner et al.</i> [2006]
SatIm11	92.5678	11.7264	90	0	25	<i>Meltzner et al.</i> [2006]
SatIm12	92.5066	11.6295	90	0	25	<i>Meltzner et al.</i> [2006]
SatIm13	92.4607	11.4766	90	0	25	<i>Meltzner et al.</i> [2006]
SatIm14	92.4556	11.3339	90	0	25	<i>Meltzner et al.</i> [2006]
SatIm15	92.4964	11.1657	90	0	25	<i>Meltzner et al.</i> [2006]
SatIm16	92.6289	11.0179	90	0	25	<i>Meltzner et al.</i> [2006]
SatIm17	92.7258	10.8905	90	0	25	<i>Meltzner et al.</i> [2006]
SatIm18	92.7462	10.7936	90	0	25	<i>Meltzner et al.</i> [2006]
SatIm19	92.7521	10.6858	90	0	25	<i>Meltzner et al.</i> [2006]
SatIm20	92.7563	10.6101	90	0	25	<i>Meltzner et al.</i> [2006]
SatIm21	92.7360	10.1463	90	0	25	<i>Meltzner et al.</i> [2006]
SatIm27	95.9867	2.97826	90	0	25	<i>Meltzner et al.</i> [2006]
SatIm28	96.0641	2.86430	90	0	25	<i>Meltzner et al.</i> [2006]
SatIm29	96.1377	2.73399	90	0	25	<i>Meltzner et al.</i> [2006]
SatIm30	96.2057	2.59235	90	0	25	<i>Meltzner et al.</i> [2006]
SatIm31	96.2454	2.47904	90	0	25	<i>Meltzner et al.</i> [2006]
SatIm32	96.2680	2.33740	90	0	25	<i>Meltzner et al.</i> [2006]
SatIm33	96.2567	2.20709	90	0	25	<i>Meltzner et al.</i> [2006]
SatIm34	96.2057	2.05412	90	0	25	<i>Meltzner et al.</i> [2006]
SatIm35	96.0471	1.78784	90	0	25	<i>Meltzner et al.</i> [2006]

Table S3: Near-field vertical offsets included in the inversion. E, eE, N, eN are defined in table S1.

Site	Lon	Lat	E(cm)	eE(cm)	N(cm)	eN(cm)	Source
ALIC	133.900	-23.700	-0.190	0.040	0.110	0.040	<i>Kreemer et al.</i> [2006]
BAHR	50.608	26.209	0.010	0.040	0.250	0.040	<i>Kreemer et al.</i> [2006]
BAKO	106.849	-6.491	0.230	0.130	0.370	0.060	<i>Kreemer et al.</i> [2006]
COCO	96.834	-12.188	0.130	0.060	0.490	0.040	<i>Kreemer et al.</i> [2006]
DARW	131.133	-12.844	-0.360	0.060	0.080	0.040	<i>Kreemer et al.</i> [2006]
DGAR	72.370	-7.270	0.540	0.060	0.600	0.040	<i>Kreemer et al.</i> [2006]
GUAM	144.868	13.589	-0.420	0.060	0.230	0.040	<i>Kreemer et al.</i> [2006]
HRAO	27.700	-25.900	0.150	0.060	-0.040	0.060	<i>Kreemer et al.</i> [2006]
HYDE	78.551	17.417	0.580	0.060	-0.140	0.040	<i>Kreemer et al.</i> [2006]
IISC	77.570	13.021	1.170	0.060	-0.110	0.040	<i>Kreemer et al.</i> [2006]
KARR	117.097	-20.981	-0.190	0.060	0.230	0.040	<i>Kreemer et al.</i> [2006]
KIT3	66.885	39.135	0.100	0.060	0.110	0.060	<i>Kreemer et al.</i> [2006]
KUNM	102.797	25.030	-0.620	0.110	-0.500	0.060	<i>Kreemer et al.</i> [2006]

Table S3: Near-field vertical offsets included in the inversion. E, eE, N, eN are defined in table S1.

LAE1	146.990	-6.670	0.190	0.080	-0.200	0.060	<i>Kreemer et al.</i> [2006]
LHAS	91.104	29.657	-0.110	0.080	-0.130	0.110	<i>Kreemer et al.</i> [2006]
MALI	40.190	-3.	0.200	0.080	0.070	0.060000	<i>Kreemer et al.</i> [2006]
MBAR	30.700	-0.600	0.140	0.060	0.050	0.040	<i>Kreemer et al.</i> [2006]
MALD	73.500	4.200	0.990	0.110	0.400	0.060	<i>Kreemer et al.</i> [2006]
NTUS	103.680	1.346	-2.200	0.060	0.800	0.040	<i>Kreemer et al.</i> [2006]
PIMO	121.078	14.636	-0.790	0.060	0.070	0.060	<i>Kreemer et al.</i> [2006]
REUN	55.600	-21.200	0.160	0.130	0.370	0.060	<i>Kreemer et al.</i> [2006]
SAMP	98.715	3.622	-13.900	0.110	-0.900	0.060	<i>Kreemer et al.</i> [2006]
SEY1	55.480	-4.670	-0.350	0.080	-0.310	0.040	<i>Kreemer et al.</i> [2006]
TNML	120.990	24.800	-0.550	0.060	-0.180	0.040	<i>Kreemer et al.</i> [2006]
TOW2	147.100	-19.300	0.160	0.060	-0.070	0.040	<i>Kreemer et al.</i> [2006]
TSKB	140.087	36.106	-0.260	0.040	-0.180	0.060	<i>Kreemer et al.</i> [2006]
WUHN	114.357	30.532	-0.390	0.060	-0.190	0.060	<i>Kreemer et al.</i> [2006]
ABGS	99.390	0.220	-0.422	0.366	-0.511	0.232	<i>Banerjee et al.</i> [2007]
ARAU	100.280	6.450	-13.025	0.914	-3.376	0.405	<i>Banerjee et al.</i> [2007]
AUCK	174.830	-36.600	-0.583	0.438	0.059	0.268	<i>Banerjee et al.</i> [2007]
BAN2	77.510	13.030	1.118	0.411	-0.334	0.268	<i>Banerjee et al.</i> [2007]
BHTW	78.600	30.800	0.089	0.286	-0.145	0.197	<i>Banerjee et al.</i> [2007]
BHUB	85.800	20.300	0.722	0.847	-0.426	0.418	<i>Banerjee et al.</i> [2007]
BNKK	100.607	13.668	-6.093	0.426	-4.255	0.261	<i>Banerjee et al.</i> [2007]
BJFS	115.890	39.610	-0.460	0.394	-0.499	0.292	<i>Banerjee et al.</i> [2007]
CHMI	98.973	18.771	-1.580	0.489	-2.490	0.296	<i>Banerjee et al.</i> [2007]
CMU	98.900	18.800	-1.404	0.695	-2.584	0.389	<i>Banerjee et al.</i> [2007]
CPN	99.400	10.700	-12.739	0.437	-6.747	0.253	<i>Banerjee et al.</i> [2007]
DAEJ	127.370	36.400	-0.234	0.396	-0.602	0.310	<i>Banerjee et al.</i> [2007]
KERG	70.256	-49.351	0.366	0.280	0.076	0.188	<i>Banerjee et al.</i> [2007]
KMI	100.800	13.700	-5.640	0.510	-4.426	0.308	<i>Banerjee et al.</i> [2007]
KUAL	103.139	5.319	-5.667	0.769	-0.559	0.412	<i>Banerjee et al.</i> [2007]
LNGG	101.160	-2.290	0.553	0.427	-0.405	0.246	<i>Banerjee et al.</i> [2007]
LUCK	80.900	26.900	0.010	0.391	-0.184	0.235	<i>Banerjee et al.</i> [2007]
MKMK	101.090	-2.540	0.606	0.437	-0.593	0.247	<i>Banerjee et al.</i> [2007]
MSAI	99.090	-1.330	0.285	0.364	-0.854	0.229	<i>Banerjee et al.</i> [2007]
NADI	76.300	32.200	0.176	0.326	0.061	0.201	<i>Banerjee et al.</i> [2007]
NGNG	99.270	-1.800	0.158	0.399	-0.794	0.236	<i>Banerjee et al.</i> [2007]
NVSK	83.240	54.840	-1.517	0.842	-0.124	0.607	<i>Banerjee et al.</i> [2007]
NYAL	11.870	78.930	0.101	0.217	0.069	0.199	<i>Banerjee et al.</i> [2007]
PBAI	98.530	-0.030	-0.629	1.819	-0.069	0.473	<i>Banerjee et al.</i> [2007]
PERT	115.885	-31.802	0.209	0.281	0.074	0.192	<i>Banerjee et al.</i> [2007]
PHKT	98.308	8.105	-23.930	0.462	-10.772	0.256	<i>Banerjee et al.</i> [2007]
POL2	74.690	42.680	-0.432	0.259	0.293	0.189	<i>Banerjee et al.</i> [2007]
PRKB	100.400	-2.970	0.128	0.431	-0.723	0.242	<i>Banerjee et al.</i> [2007]
RRLB	77.500	23.200	0.071	0.410	-0.358	0.234	<i>Banerjee et al.</i> [2007]

Table S3: Near-field vertical offsets included in the inversion. E, eE, N, eN are defined in table S1.

SHL2	91.900	25.600	-0.124	0.443	-0.245	0.268	<i>Banerjee et al.</i> [2007]
SIS2	99.867	17.157	-3.040	0.422	-3.214	0.260	<i>Banerjee et al.</i> [2007]
SUWN	127.050	37.280	-0.591	0.417	-0.302	0.328	<i>Banerjee et al.</i> [2007]
TIR0	77.	8.400	1.649	1.007	-0.186	0.376000	<i>Banerjee et al.</i> [2007]
WIH2	78.	30.300	0.069	0.274	-0.111	0.190000	<i>Banerjee et al.</i> [2007]
YAR2	115.350	-29.050	0.085	0.555	-0.049	0.352	<i>Banerjee et al.</i> [2007]
ALGO	281.929	45.956	0.116	0.246	0.533	0.467	<i>Vigny et al.</i> [2005]
BEHR	101.517	3.765	-5.591	0.279	0.231	0.188	<i>Vigny et al.</i> [2005]
BINT	113.067	3.262	-1.039	0.518	-0.617	0.232	<i>Vigny et al.</i> [2005]
FAIR	212.501	64.978	-0.377	0.328	-0.159	0.474	<i>Vigny et al.</i> [2005]
GOLD	243.111	35.425	-0.146	0.360	-0.300	0.414	<i>Vigny et al.</i> [2005]
KINA	116.039	5.905	-0.578	0.484	-0.021	0.220	<i>Vigny et al.</i> [2005]
KOKB	200.335	22.126	0.263	0.524	-0.071	0.505	<i>Vigny et al.</i> [2005]
KUAN	103.350	3.834	-3.916	0.374	0.106	0.219	<i>Vigny et al.</i> [2005]
LABU	115.245	5.283	-0.818	0.458	-0.270	0.210	<i>Vigny et al.</i> [2005]
MAC1	158.936	-54.500	-0.954	0.369	-2.319	0.509	<i>Vigny et al.</i> [2005]
MAS1	344.367	27.764	0.458	0.343	0.039	0.439	<i>Vigny et al.</i> [2005]
MKEA	204.544	19.801	0.195	0.430	0.073	0.335	<i>Vigny et al.</i> [2005]
ONSA	11.926	57.395	0.264	0.258	-0.381	0.453	<i>Vigny et al.</i> [2005]
PALP	119.906	-0.916	-0.118	0.421	0.013	0.175	<i>Vigny et al.</i> [2005]
SHAO	121.200	31.100	-0.290	0.511	-0.038	0.484	<i>Vigny et al.</i> [2005]
TOBP	120.095	-0.709	0.151	0.509	0.075	0.215	<i>Vigny et al.</i> [2005]
UNO0	116.826	-1.269	-0.365	0.471	-0.051	0.192	<i>Vigny et al.</i> [2005]
USMP	100.304	5.358	-11.513	0.478	-1.441	0.290	<i>Vigny et al.</i> [2005]
VILL	356.048	40.444	0.116	0.233	0.144	0.453	<i>Vigny et al.</i> [2005]
WATP	119.587	-0.874	-0.153	0.429	-0.098	0.180	<i>Vigny et al.</i> [2005]
YAR1	115.347	-29.047	0.086	0.410	-0.065	0.400	<i>Vigny et al.</i> [2005]
YELL	245.519	62.481	-0.023	0.270	0.028	0.428	<i>Vigny et al.</i> [2005]
UTMJ	103.640	1.566	-1.951	0.369	0.455	0.215	<i>Vigny et al.</i> [2005]
TIDB	148.980	-35.399	0.835	0.469	0.011	0.496	<i>Vigny et al.</i> [2005]
BANT	101.537	2.826	-4.501	0.393	0.347	0.245	<i>Vigny et al.</i> [2005]
GMUS	101.964	4.863	-7.052	0.458	-0.237	0.303	<i>Vigny et al.</i> [2005]
GRIK	101.130	5.439	-9.092	0.368	-1.088	0.257	<i>Vigny et al.</i> [2005]
JHJY	103.797	1.537	-1.792	0.393	0.381	0.235	<i>Vigny et al.</i> [2005]
JUIP	101.091	4.600	-7.749	0.359	-0.193	0.248	<i>Vigny et al.</i> [2005]
JUML	102.256	2.212	-2.773	0.381	0.523	0.235	<i>Vigny et al.</i> [2005]
KKBH	101.659	3.561	-5.212	0.397	0.104	0.265	<i>Vigny et al.</i> [2005]
KLUG	103.317	2.025	-2.292	0.413	0.358	0.246	<i>Vigny et al.</i> [2005]
KUKP	103.453	1.333	-1.702	0.415	0.376	0.255	<i>Vigny et al.</i> [2005]
LGKW	99.851	6.329	-14.887	0.351	-3.499	0.273	<i>Vigny et al.</i> [2005]
MERS	103.829	2.453	-2.665	0.437	0.308	0.263	<i>Vigny et al.</i> [2005]
MERU	101.407	3.138	-5.037	0.399	0.232	0.261	<i>Vigny et al.</i> [2005]
PEKN	103.390	3.493	-3.515	0.406	0.171	0.256	<i>Vigny et al.</i> [2005]

Table S3: Near-field vertical offsets included in the inversion. E, eE, N, eN are defined in table S1.

PUPK	100.559	4.207	-8.562	0.396	-0.184	0.255	<i>Vigny et al.</i> [2005]
SELM	100.695	5.217	-10.229	0.354	-1.199	0.254	<i>Vigny et al.</i> [2005]
SGPT	100.488	5.644	-11.643	0.350	-1.403	0.264	<i>Vigny et al.</i> [2005]
TGPG	104.108	1.367	-1.618	0.395	0.384	0.231	<i>Vigny et al.</i> [2005]
TLOH	102.419	3.449	-4.155	0.460	0.149	0.316	<i>Vigny et al.</i> [2005]
UPMS	101.724	2.993	-4.263	0.441	0.454	0.277	<i>Vigny et al.</i> [2005]
UUMK	100.506	6.462	-12.247	0.426	-2.310	0.312	<i>Vigny et al.</i> [2005]
SAND	118.121	5.842	-0.950	0.822	-0.602	0.337	<i>Vigny et al.</i> [2005]
TAWX	117.882	4.263	-0.564	0.980	0.198	0.373	<i>Vigny et al.</i> [2005]
BANH	99.076	10.610	-15.507	0.395	-7.482	0.237	<i>Vigny et al.</i> [2005]
CHON	101.045	13.121	-6.836	0.265	-3.835	0.203	<i>Vigny et al.</i> [2005]
NAKH	100.122	15.673	-3.938	0.412	-4.404	0.275	<i>Vigny et al.</i> [2005]
PHUK	98.304	7.759	-25.250	0.249	-10.193	0.185	<i>Vigny et al.</i> [2005]
RYNG	101.033	12.764	-7.428	0.236	-3.710	0.181	<i>Vigny et al.</i> [2005]
SRIS	104.416	14.901	-3.264	0.303	-1.800	0.218	<i>Vigny et al.</i> [2005]
UTHA	100.013	15.384	-4.715	0.236	-3.954	0.192	<i>Vigny et al.</i> [2005]
KOSG	5.810	52.178	0.104	0.186	-0.197	0.442	<i>Vigny et al.</i> [2005]
MIRI	114.002	4.372	-0.634	0.480	-0.079	0.193	<i>Vigny et al.</i> [2005]
KTPK	101.718	3.171	-4.989	0.372	0.546	0.227	<i>Vigny et al.</i> [2005]
BKPL	100.218	5.339	-13.186	0.341	-1.612	0.247	<i>Vigny et al.</i> [2005]
KLAW	102.064	2.982	-4.130	0.366	0.610	0.218	<i>Vigny et al.</i> [2005]
GETI	102.105	6.226	-8.317	0.300	-0.444	0.202	<i>Vigny et al.</i> [2005]
OTRI	99.371	18.335	-2.150	0.429	-2.310	0.238	<i>Vigny et al.</i> [2005]
KUCH	110.195	1.632	-1.307	1.342	-0.116	0.815	<i>Vigny et al.</i> [2005]